

Ph.D. THESIS

Submitted by:

MOHAMMAD SHAHID

Graduate School of Innovative Life Science

University of Toyama

Japan

THESIS TITLE

**Functional Compensation among Metabotropic
Receptors Involved in Cytosolic Ca²⁺ Signaling and
Satiety Control Mechanisms**

CONTENTS

Sr. No.	Subject	Page No.
1)	Thesis title	2
2)	Contents	3
3)	Abstract	4-5
4)	Objective	6
5)	Introduction	7-8
6)	Experimental procedures	9-14
7)	Results	15-19
8)	Discussion	20-23
9)	Figure ligands	24-26
10)	Figures	27-34
11)	References	35-37

ABSTRACT

The peptide cholecystokinin (CCK) originally described as a gut hormone secreted from duodenum (intestine) is a ubiquitous neuropeptide involved in a variety of homeostatic and physiological functions. A product of obese (Ob) gene leptin is circulating protein synthesized by the white adipose tissue. Both of these are functioning as signaling messengers involved in regulation of food intake and energy homeostasis, whereas their receptor localization, physiological interaction and functional compensation between receptors / or its receptor subtypes in the hypothalamic satiety centers are not well characterized. In the present study, we examined *fura-2* based intracellular Ca^{2+} imaging in acutely isolated mouse hypothalamic slices to analyze leptin and CCK-mediated signaling in details using gene knockout mice lacking CCK-1 receptors (CCK1R^{-/-}). The CCK receptors are categorized into two subtypes, CCK-1 and -2, both of which share a common phosphatidylinositol signaling pathway to mobilize intracellular Ca^{2+} following receptor stimulations. We focused CCK-mediated Ca^{2+} signaling in parvocellular paraventricular nucleus (PVN) cells, which control satiety and represent highest expression of CCK-1 receptors in the brain. Analysis of mouse hypothalamic slices demonstrated that the general CCK receptor agonist CCK-8s (10 nM) triggered Ca^{2+} transients most significantly in the posterior sub-region of the PVN (PaPo). This 10 nM CCK-8s-induced response was absent in CCK1R^{-/-} slices, showing that the response is mediated by CCK-1 receptors. CCK-8s concentrations higher than 30 nM triggered a Ca^{2+} rise similarly in wild-type and CCK1R^{-/-} slices. The large CCK-8s (100 nM)-induced Ca^{2+} responses in CCK1R^{-/-} slices were blocked by a CCK-2 receptor antagonist (CI-988), whereas those in wild-type slices required a mixture of CI-988 and lorglumide (a CCK-1 receptor antagonist) for complete antagonism. Therefore, CCK-1 and -2 receptors may function synergistically in single PaPo neurons and deletion of CCK-1 receptors may facilitate CCK-2 receptor signaling. This hypothesis was supported by results of real-time RT-PCR, immunofluorescence double labeling and western blotting assays, which indicated CCK-2 receptor over expression in PaPo neurons of CCK1R^{-/-} mice. Furthermore, behavioral studies showed that intraperitoneal injections of lorglumide up-regulated food accesses in wild-type but not in CCK1R^{-/-} mice, whereas CI-988 injections up-regulated food accesses in CCK1R^{-/-} but not in wild-type mice. The compensatory CCK receptor signaling shed light on currently controversial satiety-controlling mechanisms in CCK1R^{-/-} mice. Because of regular food intake activities and body weights are also reported for CCK null mutant mice, functional compensation for molecules underlying CCK-mediated satiety controls may not be limited to the two CCK receptor subtypes, and may also include other receptor signaling molecules such as leptin. So, we further extended our study focused on leptin and CCK signaling in hypothalamic neurons. Our preliminary data based on Ca^{2+} imaging and real time RT-PCR assay indicated that leptin and

CCK-1 receptor signaling were synergistically interacted in PVN neurons as in the case of CCK-1 and -2 receptors. These results suggested receptor-wide as well as subtype-wide compensatory mechanisms in the regulation of satiety via metabotropic receptors.

OBJECTIVE

Functional compensation between cholecystokinin-1 and 2 receptors in murine paraventricular nucleus neurons

INTRODUCTION

Cholecystokinin (CCK) peptide, originally described as a gut hormone (Ivy and Oldberg, 1928; Mutt and Jorpes, 1968), is currently recognized as a ubiquitous neuropeptide enrolling numbers of homeostatic and physiological functions, including neuroendocrine regulation (Bondy et al., 1989), satiety controls (Gibbs et al., 1973; Antin et al., 1975), pain transmission (Baber et al., 1989), and learning and memory (Itoh and Lal, 1990), yet receptor localizations and functions are largely unknown.

For the satiety controls, CCK peptides secreted from the gastrointestinal tract in response to ingestion indirectly control hypothalamic satiety centers such as the paraventricular nucleus (PVN) and dorsal medial hypothalamus (DMH), via a large scale afferent network including the nervus vagus and the medullary nucleus tractus solitarius (NTS) (Rinaman et al., 1993; Mönnikes et al., 1997; Reidelberger et al., 2003, 2004; Bi et al., 2004). Of the two subtypes of CCK receptors, CCK-1 receptors are believed to play a pivotal role for satiety controls, since (i) CCK-1 receptors are expressed both in the nervus vagus and the hypothalamic satiety centers (Honda et al., 1993; Wei and Wang, 2000; Bi et al., 2004; Shimazoe et al., 2008), (ii) administrations of CCK-1 agonists, but not CCK-2 agonists reduced ingestion (Moran et al., 1992; Simmons et al., 1999), and (iii) larger meal size and obese were observed in a mutant rat strain, Otsuka Long Evans Tokushima Fatty (OLETF), which lacks CCK-1 receptor genes (Takiguchi et al., 1997; Moran et al., 1998). Based on these, CCK-1 agonists are currently a target for drug developments to treat overweight and obesity (Szewczyk and Laudeman 2003; Berna et al., 2007; Cawston and Miller 2010).

Principal targets of peripheral CCK to control satiety responses may be receptors located in the gut (Raboin et al., 2008; Washington et al., 2010) and vagal afferents (Smith et al., 1981, 1985) which terminate on the NTS. The NTS may use glutamate as an essential neurotransmitter to convey ascending satiety signals to the brain (Appleyard et al., 2007; Guard et al., 2009). However, NTS cells also contain CCK peptides and CCK-1 receptors (Kiyama et al., 1983; Takagi et al., 1984; Broberger et al., 2001) to facilitate glutamatergic neuronal transmissions (Appleyard et al., 2007). Within the brain, the PVN and DMH, or other hypothalamic centers involved in food intake behaviors receive CCK peptides not only from the NTS but also from neighboring neurons for the integration of various signaling inputs. For example, PVN neurons, which contain high levels of CCK peptides, upregulate transcriptional levels of CCK-1 and -2 receptor genes following osmotic stress presentations (Hinks et al., 1995). In addition, the hypothalamic suprachiasmatic nucleuses, the center of biological clock,

contain CCK peptides (Van den Pol and Tsujimoto 1985; Silver et al., 1999) and send axons to the PVN and DMH (Aston-Jones et al., 2001). Therefore, PVN circuits, including CCK-mediated satiety controlling mechanisms, may undergo circadian clock regulations. Centrally administered CCK was sufficient to produce satiety response and this response was mediated by CCK-1 but not CCK-2 receptors (Crawley et al., 1991; Hirose et al., 1993). Therefore, analysis regarding localizations and functions of CCK-1 receptors in the brain is inevitable for the complete understanding of satiety systems.

Previous study of ours visualized CCK-1 receptor gene expressions in the several hypothalamic nuclei involved in food intake behaviors, including PVN, DMH, ventral medial hypothalamus, and arcuate nuclei with the largest expression found in the posterior subregion of PVN (PaPo) (Shimazoe et al., 2008) whereas CCK1R^{-/-} mice are known to display normal feeding behaviors and body weight (Kopin et al., 1999; Takiguchi et al., 2002). The PaPo represented satiety-dependent cFos and oxytocin gene expressions (Uchoa et al., 2009) and fasting-dependent estrogen receptor immunoreactivities (Panicker et al., 1998) whereas the locus has been highlighted neither for CCK signaling nor for satiety controls. Therefore, the present study examined intracellular Ca²⁺ imaging in mice PVN slices to analyze the CCK signaling in details. In addition, CCK-1 and -2 receptor expressions were analyzed by the real-time RT-PCR in several brain regions in the wild type and CCK1R^{-/-} mice. Since we observed compensatory gene expressions and synergic functions between CCK-1 and -2 receptors in PaPo cells, we further investigated the effect of CCK-2 antagonist on feeding behaviors in CCK1R^{-/-} mice.

EXPERIMENTAL PROCEDURES

Mice—

Mice bred under a light-dark cycle (light on 08:00-20:00) at a constant temperature (22 ± 1 °C) were used in all experiments. Male CCK1R^{-/-} mice and their wild-type control littermates were generated as described previously (Takiguchi et al., 2002; Shimazoe et al., 2008). In short, a targeting vector was designed to replace the Sal/I-BglII 1.9-kb genomic fragment of the mouse CCK-1 receptor gene with NLS-lacZ and pGK-neo cassette. The homologous recombination deleted the first 122 amino acids, including the first membrane-spanning region of the CCK-1 receptor. J1 embryonic stem cells were electroporated with the targeting vector and selected with G418 on embryonic fibroblast feeder cells. After Southern blot analysis screening, the successful ES clones were microinjected into blastocysts of C57BL/6J females. Two independent ES clones generated germline chimeras. The chimeras were bred with C57BL/6J mice to generate heterozygous CCK1R^{+/-} mutant F1 mice. CCK1R^{-/-} mice were finally generated by mating CCK1R^{+/-} mice followed by sufficient backcross to C57BL/6J wild-type mice. Experiments below were approved by the Committee of Animal Care of University of Toyama, Japan.

5-bromo-4-chloro-3-indolyl- β -D-galactopyranoside (X-gal) staining—

2-3 months old male CCK1R^{+/-} mice were deeply anesthetized with an intraperitoneal (*i.p.*) injection of sodium pentobarbital (50 mg/kg) and transcardially perfused with phosphate buffered saline (PBS) for 5 min followed by ice-cold 4% paraformaldehyde in 0.1 M phosphate buffer for 15 min. Whole brains were removed and further fixed in the same fixative (4 °C, overnight). Then, olfactory bulbs and/or cerebellums were cut from the brain in ice-cold PBS. Pre-trimmed brains were immersed in 30% sucrose PBS and stored overnight at 4 °C. The fixed and cryoprotected brains were embedded with O.C.T. compound (Sakura Finetek, Tokyo, Japan). Frozen sections of 50 μ m thickness were cut using a cryostat microtome and washed three times with PBS in 24-well plates, after which they were mounted on glass slides. The samples were then stained for 7 h at 37 °C with an X-gal staining kit (K1465-01, Invitrogen, Carlsbad, CA) according to the manufacturer's instructions. These samples were thoroughly washed with PBS and then embedded with 70% glycerol (Wako Pure Chemical Co., Osaka, Japan) dissolved in PBS. These samples were imaged using a color charge-coupled device (CCD) camera (Ds-5Mc, Nikon, Tokyo, Japan) mounted on an inverted microscope (TE-2000, Nikon).

Immunostaining for β -galactosidase—

Brain sections (30 μ m thickness) as above were used for immunofluorescence staining. The fixed sections were rinsed 3 times with PBS and then incubated in blocking solutions containing 10% donkey serum (Jackson Immuno Research Laboratories, West Grove, PA) and 0.1% Triton-X 100 (Sigma, St. Louis, MO) for 24 h at 4 °C. Then, samples were incubated with 1:2000 mouse anti- β -galactosidase (Sigma) dissolved in PBS containing 5% donkey serum and 0.05% Triton-X 100 for 48 h at 4 °C. After three 15-min PBS rinses, samples were incubated in 1:200 Cy3-conjugated donkey anti-mouse IgG (Jackson). After five 20-min PBS rinses, samples were incubated with 1:1000 4,6-diamidino-2-phenylindole (DAPI) (Dojindo Laboratories, Kumamoto, Japan) dissolved in PBS for 20 min at room temperature (22-26 °C). These samples were thoroughly washed with PBS and then embedded with Elvanol polyvinyl alcohol. The fluorescent images were acquired using a monochromatic cooled CCD camera (Ds-2MBWc, Nikon), 100W Xenon lamp, and standard FITC/Cy3 filter sets mounted on an inverted microscope (TE-2000, Nikon). Digital images were processed using PhotoShop 6.0 software (Adobe Systems, San Jose, CA).

Immunostaining for CCK receptors—

Slice cultures were prepared from the posterior part of PVN (PaPo) of 2-3-days-old wild type (+/+) and CCK1R^{-/-} (-/-) mice. Coronal hypothalamic slices containing the PaPo were cut using a vibrating-blade microtome in artificial cerebrospinal fluid (ACSF) containing 138.6 mM NaCl, 3.35 mM KCl, 21 mM NaHCO₃, 0.6 mM NaH₂PO₄, 9.9 mM d-glucose, 0.5 mM CaCl₂, and 3 mM MgCl₂, that was filtered through a 0.22 μ m membrane filter and bubbled with 95% O₂ and 5% CO₂. These slices were trimmed to an approximately 4 \times 4 mm square containing the PaPo of the hypothalamus centered on the third ventricle. The slices were placed in a 0.40 μ m filter cup (Millicell-CM, Millipore, Bedford, MA). All these procedures were completed within 15 min at 4 °C under sterile conditions. The filters were placed in a standard 6-well plate and cultured with 1 ml of medium consisting of 50% Eagle's basal medium, 25% Earle's balanced salt solution, and 25% heat-inactivated horse serum supplemented with 5 mg/ml glucose and 1:100 Glutamax (GIBCO BRL). The cultures were maintained in a CO₂ incubator at 35.5 °C \pm 0.5 °C and 5% CO₂. The medium was changed every 3–4 days. The slice containing the PaPo was used for two-step double immunofluorescence staining for CCK1Rs and -2Rs. The staining was performed using antibodies against CCK1Rs (CCK-AR (N-20) antibody, sc-16172, Santa Cruz Biotechnology, CA) and CCK2Rs (gastrin receptor polyclonal antibody, bs-1777R, Bioss, MA). Slices were fixed with 4% paraformaldehyde in PBS at pH 7.4 for 5 min. The samples were rinsed three times with PBS and incubated in blocking solutions containing 10% donkey serum and 0.05% Triton-X 100 for 24 h at 4 °C to block nonspecific

antibody binding. Samples were then incubated for 48 h at 4°C with 1:100 rabbit anti-CCK2R antibody dissolved in PBS containing 5% donkey serum. After three 15-min PBS rinses, the samples were incubated with 1:200 Cy3-conjugated donkey anti-rabbit IgG antibody overnight (< 20 h) at 4°C. Following five 20-min rinses with PBS, the sample was incubated with 1:200 goat anti-CCK1R antibody dissolved in PBS containing 5% donkey serum. After three 15-min PBS rinses, the samples were incubated with 1:200 Alexa647-conjugated donkey anti-goat IgG (Jackson) antibody overnight at 4°C. Following five 20-min rinses with PBS, samples were incubated with 1:1000 DAPI solutions. The samples were thoroughly washed with PBS and then embedded with Elvanol polyvinyl alcohol. Immunofluorescence images were viewed using a confocal imaging system equipped with an inverted microscope, UPLSAPO 60×NA1.35 oil immersion objective lens, and argon/helium neon lasers (Fluoview 1000, Olympus, Tokyo, Japan). Scanning parameters were unified across specimens.

Ca²⁺ imaging in acutely-isolated brain slices—

Coronal hypothalamic slices (200-220 μm thickness) containing the PVN were prepared following deep pentobarbital anesthesia in male mice of postnatal day 12-15 using a vibrating blade microtome in ice-cold high-Mg²⁺ artificial cerebrospinal fluid (aCSF) containing (in mM) NaCl, 138.6; KCl, 3.35; NaHCO₃, 21; NaH₂PO₄, 0.6; D-glucose, 9.9; CaCl₂, 0.5; MgCl₂, 4, and bubbled with 95% O₂/5% CO₂. Three to four sequential slices were prepared from each mouse brain and placed separately on 7×7 mm 12 μm membrane filters (Nuclepore, Cambridge, MA). The slices were incubated at room temperature for 1-8 h in regular aCSF (2.5 mM CaCl₂ and 1 mM MgCl₂) bubbled with 95% O₂/5% CO₂. For Ca²⁺ imaging, the slices were placed in a 0.40 μm filter cup (30 mm diameter; Millicell-CM, Millipore, Bedford, MA) and immersed for 45-60 min in 1.5 mL of regular aCSF containing 10 μM fura-2 AM (Dojindo Laboratories) and 0.01% Pluronic (Invitrogen). During the entire staining procedure, the staining solution was gently bubbled with 95% O₂/5% CO₂ through a stainless steel pipe located outside the cup filter. After washing out the staining solution with aCSF and incubating for an additional 30 min, the slice was gently removed from the holding membrane filter and placed in a glass-bottomed microscope stage chamber (0.5 mL) for optical measurements.

Fluorescence images were observed using an upright microscope (Axioskop; Carl Zeiss, Thornwood, NY) with a water-immersion objective (Achromplan×40 NA0.75, Carl Zeiss). The wavelength of the excitation UV light (340 nm or 380 nm pulse; 100 msec) was switched using a filter wheel (Lambda 10-2; Sutter Instruments, Novato, CA). The UV light was generated by a full-spectrum 175W Xenon bulb (Lambda LS; Sutter), conducted to the microscope through a liquid light guide and reflected using a dichroic mirror (FT 395 nm; Carl Zeiss). The pair of fluorescent images was processed using a band-pass filter (BP 485-515 nm;

Carl Zeiss) and exposed to a multiple format cooled CCD camera (CoolSnap-fx; Photometrics, Tokyo, Japan) at 6-second intervals. The filter wheel and the CCD camera were controlled using digital imaging software (MetaFluor ver. 6.0; Japan Molecular Devices, Tokyo, Japan). The background fluorescence was also subtracted using the software. During recording, slices were placed in a 0.5 mL bath chamber and perfused with aCSF at a flow rate of 2.5 mL/min. Until otherwise noted, the aCSF contained tetrodotoxin (TTX; 0.5 μ M, Sankyo Co., Tokyo, Japan) throughout the experiments. The CCK-8s (Sigma), lorglumide (LGM; LKT Laboratories Inc., St. Paul, MN), thapsigargin (Sigma), CCK-4 (Peptide Institute, Osaka, Japan), CI-988 (Tocris, Bristol, UK), and glutamate (Wako) were applied by switching the perfusate. Glutamate stimulation was used as a positive control for the neuronal responses because about 75% of PVN cells with neuronal cell shapes (excluding larger astroglial cells) increased Ca^{2+} by the bath application of 100 μ M glutamate.

Real time reverse transcription polymerase chain reaction (RT-PCR) assay—

Male wild-type and CCK1R^{-/-} mice of 2 month old were deeply anesthetized with an *i.p.* injection of sodium pentobarbital (50 mg/kg). Whole brains were then removed and directly frozen on a dry ice. Frozen brains were transferred to a cryostat chamber at -30 °C, mounted with O.C.T. compound at -15 °C and sectioned at 100 μ m thickness. Frozen sections were transferred on a glass slide, punched out with flat-top stainless pipettes (inner diameter, 0.33 mm; hand-made from 23G disposable syringe tips) on ice and homogenized by a bio-masher (Funakoshi, Tokyo, Japan) with 600 μ l buffer RLT (RNeasy kit, Qiagen, Chartsworth, CA) at 2,500 rpm for 30 sec. Following the addition of 600 μ l 70% ethanol, samples were stored at -80 °C.

Total RNA (4 μ g for each sample) was extracted from a tissue homogenate using the RNeasy kit according to the manufacturer's instructions. Reversed transcription, including DNase treatment, was processed using a QuantiTect reverse transcription kit (Qiagen) with a standard procedure. PCR primer were designed as follows: CCK-1 receptor forward primer, GACAGCCTTCTTATGAATGGGAG; CCK-1 receptor reverse primer, GCTGAGGTTGATCCAGGCAG; CCK-2 receptor forward primer, GATGGCTGCTACGTGCAACT; CCK-2 receptor reverse primer, CGCACCACCCGCTTCTTAG; β -actin forward primer, AGTGTGACGTTGACATCCGTA; β -actin reverse primer GCCAGAGCAGTAATCTCCTTCT. The real-time PCR was performed using the Rotor Gene 3000A system (Corbett Research, Mortlake, NSW, Australia) with a 72-well rotor. The PCR reactant consisting of template cDNA, 2 \times Roter-Gene SYBR Green, forward and reverse primers (50 μ M, each), and RNase-free water in a 0.1 ml strip tube received following temperature steps; initial PCR activation at 95 °C for 5 min and 60 thermal cycles

consisting with 95 °C for 5 sec and 60 °C for 10 sec. Reactions in 4 separate tubes were averaged for each sample.

The amount of gene product in each sample was determined by the comparative quantification method using the Rotor Gene 6.0 software (Corbett Research). The amount of gene product for the gene of interest was expressed relative to that of β -actin to normalize for differences in total cDNA between samples.

Western Blotting—

Wild-type and CCK1R^{-/-} mice aged 2 months were deeply anesthetized with an intraperitoneal injection of sodium pentobarbital (50 mg/kg). Whole brains were removed and sliced as described above for Ca²⁺ imaging analysis. Hypothalamic nuclei were trimmed on ice and homogenized in 1:100 ratio of protease inhibitor mixture (Sigma) and cell lysis solution (50 mM Tris-HCl, pH 7.5, 0.15 M NaCl, 0.1% SDS, 1% Triton X-100, 1% sodium deoxycholate) using a biomasher (Funakoshi). Microsomal proteins were spun down by centrifugation at 15,000 g for 2x20 min at 4 °C. The supernatants were used for standard western blotting assays. Proteins were resolved by SDS-PAGE (10% acrylamide Mini-PROTEAN TGX Gel; Bio-Rad) and electroblotted onto 0.45-m nitrocellulose membranes (Bio-Rad). Membranes were blocked for 1 h at room temperature with 5% Block-Ace (DS Pharma Biomedical, Osaka, Japan) in detergent-supplemented Trisbuffered saline (TBS-T; 20 mM Tris, 150 mM NaCl, 0.05% Tween 20, pH 7.5). Membranes were subjected to rabbit polyclonal CCK2R antibody (1:200) (Santa Cruz Biotechnology) and rabbit polyclonal GAPDH antibody (1:400) (Santa Cruz Biotechnology) in TBS-T overnight at 4 °C, washed in TBS-T (5 10 min), then incubated for 1 h with HRP-conjugated donkey anti-rabbit IgG (1:50,000) (Jackson) in TBS-T. After extensive washing (6 10 min) with TBS-T using a rotor shaker, membranes were subjected to luminal reactions using standard procedures (Immun-Star Western C kit; Bio-Rad laboratories). Luminescence intensity was quantified using a monochromatic cooled CCD system installed in a black box (E-Z capture II; Atto Biotechnology, Japan).

Behavioral analysis—

Male wild type mice and CCK1R^{-/-} mice of 2 month old were individually housed in originally designed acrylic chambers (H35×W17×D25 cm) in which food-accesses were detected by a touch sensor (PS-306, Elekit, Fukuoka, Japan). The sensing probe was connected to a standard stainless pellet server. Since the bottom of the pellet server was placed 5 cm above nesting chips, purposeful food access behaviors but not general locomotor activities were counted by this system. The ON/OFF signals from the sensor were fed into a laptop computer through a photo-coupler isolated digital I/O card (PIO-16/16L, Contec Inc. Tokyo, Japan) and

automatically counted at a 3 minute interval by software written by M.I.

To analyze effects of CCK receptor antagonists on food intake behaviors, wild type (n = 14) and CCK1R^{-/-} (n = 14) were individually reared in the recording cages under standard light-dark cycles (light on 08:00-20:00) and received daily *i.p.* injections of sterilized saline (90 μ l) at 19:30-20:00 for 5 days. Subsequently, the injectant was replaced to 5% DMSO in sterilized saline (vehicle) on the sixth day and to CI-988 (2 mg/kg, dissolved in the vehicle) or LGM (2 mg/kg, dissolved in the vehicle) on the seventh day.

Statistical analysis—

Data are presented as means with standard error. One way analysis of variance (ANOVA) followed by Duncan's multiple range tests were used for the statistical comparison across multiple means. Two-tailed Student's *t*-test was used for the pair wise comparisons. A 95% confidence level was considered to indicate statistical significance.

RESULTS

Localization of CCK-1 receptor gene expression in the hypothalamic PVN

To visualize localization of CCK-1 receptors in the PVN, the present study used X-gal staining and β -galactosidase (β -gal) immunostaining for series of hypothalamic sections prepared from the CCK1R \pm mice (Fig. 1). Within the sections analyzed, the PaPo displayed larger staining levels than anterior-to-medial PVN or other nuclei enrolling satiety controls (Fig. 1A). Total number of immunoreactive cells counted within approximate PVN boundaries in the posterior sections (including PaPo) was 3.3 times higher than those in the medial PVN and 9.3 time higher than those in the anterior PVN ($F_{2,6} = 349$, $P < .01$; Fig 1C). This difference did not depend on the general cell density since largest counter staining was observed in the medial PVN (Fig. 1B). The cell population ratio which represented β -gal-immunoreactivity in the posterior PVN ($28.4 \pm 0.6\%$) was 6-7 times higher than that in the anterior-to-medial PVN ($F_{2,6} = 641$, $P < .01$; Fig. 1D).

Localization of CCK-1 receptor-mediated intracellular Ca^{2+} mobilization in the hypothalamic PVN

To further visualize functional CCK-1 receptor distributions in the PVN, the present study examined *fura-2*-based Ca^{2+} imaging experiments for acutely isolated hypothalamic slices. The PVN slices were stimulated briefly with 10 nM CCK-8s under circulation of aCSF. Most of the PVN cells increased intracellular Ca^{2+} concentration ($[Ca^{2+}]_i$) (33 out of 81 cells; $40.3 \pm 2.3\%$, number of slices = 4) with a few exception which rather decreased $[Ca^{2+}]_i$. The inhibitory action of CCK-8s was completely blocked by TTX supplement in aCSF, indicating indirect response via inhibitory inter-neurons. Therefore, the later studies aim to analyze local Ca^{2+} responses were conducted with TTX supplement.

Within sequential hypothalamic slices, cells represented CCK-8s (10 nM)-induced Ca^{2+} increase were located preferentially in the posterior PVN (Fig. 2A). Responsive cell ratio in the posterior PVN ($43.4 \pm 2.7\%$, number of slices = 6) was 3.3 times higher than that in the anterior PVN and 1.9 times of that in the medial PVN ($F_{2,15} = 63.41$, $P < .01$). The CCK-8s (10 nM)-induced Ca^{2+} response was triggered by CCK-1 receptors since the response was negligible in slices prepared from the CCK1R \pm mice ($< 1.5\%$; number of slices = 6 for each PVN area; Fig. 2A).

Genotype, dose, and time of day-dependent Ca^{2+} increase via CCK-8s in PaPo cells

The dose-response of CCK-8s induced Ca^{2+} rise was studied in PaPo cells prepared from the wild type and CCK1R \pm mice. The CCK1R \pm cells displayed no apparent Ca^{2+}

elevations at 10 nM whereas displayed Ca^{2+} increase similar to the wild type cells at 100 nM (Fig. 2B). Accordingly, the EC_{50} was estimated at 15.2 nM for the wild type and 48.7 nM for CCK1R^{-/-} cells (Fig. 2C).

Day-night variations in responsive cell populations were also analyzed in the wild type slices. For the daytime analysis, slices were cut early in the morning and monitored during the middle of the daytime (12:00-16:00). For the nighttime analysis, slices were cut late afternoon and monitored during the mid night (00:00-04:00). Larger number of the cells responded to 10 nM CCK-8s during the nighttime than during the daytime (+8.8%, $P < .05$). However, the day-night differences were not observed in 100 nM CCK-8s or glutamate responses (Fig. 2D).

Co-expression and functional synergy between CCK-1 and -2 receptors in PaPo neurons

To estimate cellular machinery underlying CCK-8s-induced Ca^{2+} responses in PaPo cells, repeated CCK-8s stimulations were examined with different extracellular buffers. First, CCK-8s (10 nM) stimulations in the wild type slices were conducted with circulation of Ca^{2+} -free aCSF. However, neither the amplitude of Ca^{2+} rises ($\Delta[\text{Ca}^{2+}]_i = 0.062 \pm 0.003$, number of cells = 27 for controls and $\Delta[\text{Ca}^{2+}]_i = 0.061 \pm 0.003$, number of cells = 25 for Ca^{2+} -free buffer) nor the population of CCK-8s responses ($40.7 \pm 1.8\%$ for controls and $37.5 \pm 2.4\%$ for Ca^{2+} -free buffer; number of slices = 4; N.S.) were reduced by Ca^{2+} -free buffer. On the other hand, the CCK-8s (10 nM) response was completely abolished after thapsigargin depletion of internal Ca^{2+} stores ($40.3 \pm 1.7\%$ for controls and 0% after thapsigargin treatment; number of slices = 4). These results clearly indicate that CCK-8s (10 nM) triggered release of Ca^{2+} from internal Ca^{2+} stores in wild type PaPo cells (Fig. 3A).

Similar to these responses, CCK-8s (100 nM)-induced Ca^{2+} responses in CCK1R^{-/-} slices were also resistant to Ca^{2+} -free buffer ($\Delta[\text{Ca}^{2+}]_i = 0.082 \pm 0.002$, number of cells = 23 for controls and $\Delta[\text{Ca}^{2+}]_i = 0.08 \pm 0.002$, number of cells = 22 for Ca^{2+} -free buffer; N.S.). The responsive cell populations were also not statistically different in the Ca^{2+} -free buffer ($39.5 \pm 1.1\%$ for controls and $37.4 \pm 1.6\%$ for Ca^{2+} -free buffer; number of slices = 4; N.S.) but were completely abolished after thapsigargin treatments ($41.6 \pm 2.1\%$ for controls and 0 % after thapsigargin treatment; number of slices = 4). Therefore, both of these CCK-8s responses may depend on release of Ca^{2+} from internal Ca^{2+} stores (Fig. 3B).

To further characterize mechanisms underlying CCK-8s-induced Ca^{2+} responses in PaPo cells, we examined effects of CCK antagonists on these responses. First, wild type PaPo cells were repeatedly stimulated with CCK-8s (10 nM) or CCK-4 (100 nM), the specific agonist for CCK-2 receptors (Figs. 4A, B). The CCK-8s (10 nM)-induced Ca^{2+} transients were strongly blocked by LGM (10 μM); a CCK-1 receptor antagonist ($\Delta[\text{Ca}^{2+}]_i = 0.06 \pm 0.003$ for controls

and $\Delta[\text{Ca}^{2+}]_i = 0.009 \pm 0.001$ under LGM treatments; number of cells = 30 in four slices, $P < .01$; Fig. 4A *middle*). The CCK-4 (100 nM) similarly evoked Ca^{2+} transients in PaPo cells (responsive cell populations = $41.3 \pm 3\%$, number of slices = 4) and the response was completely blocked by CI-988, a CCK-2 receptor antagonist (Fig. 4B). These results denote CCK-1 and -2 receptor functions in the PaPo and theoretical antagonistic activities of LGM and CI-988 for these receptors.

Subsequently, repeated stimulations by large CCK-8s (100 nM) were examined in the presence of LGM and CI-988 (Figs. 4C, D). In the wild type slices, the large CCK-8s-induced Ca^{2+} transients were partially blocked by 10 μM LGM ($\Delta[\text{Ca}^{2+}]_i = 0.091 \pm 0.004$, number of cells = 34 for controls and $\Delta[\text{Ca}^{2+}]_i = 0.048 \pm 0.003$, number of cells = 31 under LGM treatments; $P < .01$; Fig. 4C *middle*) or by 1 μM CI-988 ($\Delta[\text{Ca}^{2+}]_i = 0.088 \pm 0.003$, number of cells = 36 for controls and $\Delta[\text{Ca}^{2+}]_i = 0.047 \pm 0.002$, number of cells = 33 under CI-988 treatments; $P < .01$; Fig. 4C *right*), whereas commixture of these antagonists completely blocked the Ca^{2+} transients (Fig. 4C, *left*). On the other hand, the large CCK-8s-induced Ca^{2+} transients in CCK1R^{-/-} slices were almost completely blocked by CI-988 alone ($\Delta[\text{Ca}^{2+}]_i = 0.079 \pm 0.002$, number of cells = 32 for controls and $\Delta[\text{Ca}^{2+}]_i = 0.007 \pm 0.001$, number of cells = 29 under CI-988 treatments; $P < .01$; Fig. 4D *right*) whereas LGM failed to blocked the responses (number of slices = 4; Fig. 4D *middle*). The mean $\Delta[\text{Ca}^{2+}]_i$ caused by the large CCK-8s in CCK1R^{-/-} slices reached 91% of that in the wild type slices although the size is statistically different ($\Delta[\text{Ca}^{2+}]_i = 0.089 \pm 0.001$, number of cells = 143 for the wild type and $\Delta[\text{Ca}^{2+}]_i = 0.081 \pm 0.001$, number of cells = 134 for CCK1R^{-/-} slices; $P < .01$; Figs. 4C, D). In addition, the mean $\Delta[\text{Ca}^{2+}]_i$ caused by the large CCK-8s in CCK1R^{-/-} slices was 33% larger than the CCK-4 (100 nM)-induced Ca^{2+} transients in the wild type slices ($\Delta[\text{Ca}^{2+}]_i = 0.061 \pm 0.001$, number of cells = 126; $P < .01$; Figs. 4B, D). These results thus indicate (i) co-expression of CCK-1 and -2 receptors in single PaPo cells and (ii) upregulation of CCK-2 receptors by CCK1R^{-/-}.

Consequently, dose-response curves for CCK-8s-induced Ca^{2+} mobilizations were re-analyzed for PaPo cells under LGM or CI-988 treatment (Fig. 5). In the wild-type cells, CCK-8s EC_{50} under LGM treatments (i.e., net CCK2R response; 55.4 nM) was 4.5-fold that under CI-988 treatments (net CCK1R response; 12.2 nM). By CCK1R^{-/-}, CCK-8s EC_{50} under LGM treatments in CCK1R^{-/-} cells was slightly reduced (0.78-fold wild-type level; 43.2 nM) and maximal amplitude was significantly amplified (1.74-fold wild-type level). These results indicate elevated affinity and efficacy of CCK2Rs by CCK1R^{-/-}.

Compensatory CCK-2 gene expression in CCK1R^{-/-} mice

Transcriptional activities of genes encoding CCK-1 and -2 receptors were studied

using a real-time RT-PCR for the tissue punch outs of PVN subregions and other brain regions regulating satiety. Relative abundance of CCK-1 receptor mRNA in the posterior PVN was 3.7 times that in the anterior PVN and 1.6 times that in medial PVN ($F_{2,9} = 6.0$, $P < .01$; Fig. 6A). The level of CCK-1 receptor mRNA expressions in the posterior PVN was largest among the all brain regions analyzed in the present study ($F_{6,21} = 6.1$, $P < .01$). On the other hand, CCK-2 receptor mRNA was ubiquitous and the abundance displayed no statistical differences within the PVN subregions ($F_{2,9} = 1.7$, N.S.). The abundance of CCK-2 receptor mRNA was twice as much as the wild type levels in anterior PVN ($P < .05$), medial PVN ($P < .01$), posterior PVN ($P < .01$) and NTS ($P < .01$). The tendency of CCK-2 receptor mRNA increase in CCK1R^{-/-} mice was also observed in the ventromedial hypothalamus (1.5 times of wild type levels) and the arcuate nucleus (1.4 times of wild type levels) whereas these differences were not statistically significant (Fig. 6B). These results indicate compensatory CCK-2 receptor gene expressions in CCK1R^{-/-} mice depending on the brain regions.

Co-expression and Compensatory Expression of CCK1R and CCK2R Proteins in PVN Neurons—

The above series of evidence denotes compensatory expression and functional synergy between CCK1R and -2R in PVN neurons; we confirmed this by immunofluorescence staining and Western blotting studies. Because visualization of plasma membrane receptor immunoreactions in cryostat sections was difficult, we used organotypic slice cultures in which live neurons were located on thin slice surfaces to visualize cellular localization of receptor proteins. Within the PVN, the CCK1R antibody successfully recognized the subpopulation of parvocellular PVN neurons where signals were found both in cell bodies and dendrites (Fig. 7A). CCK2R antibody recognized much larger cell populations in the PVN (Fig. 7A). Most CCK1R-immunoreactive (-ir) cells overlapped with CCK2R-ir cells (62 of 64 cells in four slices), demonstrating co-localization of CCK1R and -2R in PVN neurons. Consistent with the transcriptional levels, Western blotting analysis clearly demonstrated up-regulation of CCK2R protein levels in the PVN of CCK1R^{-/-} mice (2.4-fold wild-type levels; $P < .01$; Fig. 7B). Nevertheless, the number of CCK2R-ir cells was not increased by CCK1R^{-/-} (cell density = 30.8 ± 1.5 /field for the wild-type and 32.3 ± 2.5 /field for CCK1R^{-/-}, Fig. 7A). This indicates that compensatory expression of CCK2R occurred in cells that originally express CCK2R, including CCK1R-positive cells, although the CCK2R-ir intensity was equalized by image processing using confocal scanning microscopy.

Functional compensation between CCK-1 and -2 receptors for satiety controls

To analyze whether the functional compensations between two CCK receptor subtypes

could influence at systems level, effects of CCK antagonists on food access behaviors were monitored in the wild type and CCK1R^{-/-} mice. The wild type and CCK1R^{-/-} mice displayed similar food intake behaviors, high during the nighttime (mean number of food accesses = 1074 ± 29 for the wild type and 1090 ± 22 for CCK1R^{-/-} mice, n = 14 for each genotype; N.S.) and low during the daytime (mean number of food accesses = 165 ± 22 for the wild type and 157 ± 8 for CCK1R^{-/-} mice, n = 14 for each genotype; N.S.; Figs. 8A, B). The *i.p.* injection of LGM (2 mg/kg) at dark onset facilitated successive nighttime food accesses only in the wild type mice (+11.1% of vehicle injected controls; $F_{3,28} = 4.9$, $P < .01$) but not in CCK1R^{-/-} mice (+3.8% of vehicle injected controls; N.S.; Fig. 8C). On the other hand, *i.p.* injection of CI-988 (2 mg/kg) at dark onset facilitated successive nighttime food accesses only in CCK1R^{-/-} mice (+15.0% of vehicle injected controls; $F_{3,20} = 3.4$, $P < .05$) but not in the wild type mice (+0.8% of vehicle injected controls; N.S.; Fig. 8D). These results indicate that CCK-1 receptor signaling for the satiety control was switched to CCK-2 receptor signaling in CCK1R^{-/-} mice.

DISCUSSION

The present study analyzed CCK receptor functions in mice hypothalamic slices using Ca^{2+} imaging techniques and demonstrated significant CCK receptor functions in the PaPo. Localized CCK-8s-induced Ca^{2+} response are consistent with reporter gene identification of CCK-1 receptor expressions. In PaPo neurons, both CCK-1 and -2 receptors may involve endogenous CCK signaling, since synergic contribution of CCK-1 and -2 receptors was observed for CCK-8s (≥ 30 nM)-induced Ca^{2+} mobilizations. The substitutive CCK-2 receptor gene expression revealed by the real-time RT-PCR assay and western blotting explains compensatory CCK-2 receptor functions in the PaPo of CCK1R^{-/-} mice. CI-988 injection activated food access behaviors in CCK1R^{-/-} mice but not in the wild type mice, further suggesting the functional compensation between CCK-1 and -2 receptors at systems level. It has been widely shown that pharmacological blockage of CCK-1 receptors reduces satiety and facilitates feedings and CCK-1 agonists are candidate drugs to treat overweight and obesity. On the other hand, conventional gene knockout mice lacking CCK-signaling not always follow these pharmacological evidences, resulting in controversial interpretations in satiety controlling mechanisms. Thus, functional compensation between CCK-1 and -2 receptors observed in the present study will answer the inconsistency and shed light on the mechanisms underlying CCK-mediated satiety controls.

The PaPo as a center for CCK-1 receptor-mediated autonomic controls

The hypothalamic PVN is an important integrating site for autonomic and endocrine function (Swanson & Sawchenko, 1980). This nucleus is a heterogeneous neuronal cluster consisting of magnocellular and parvocellular neurons that are largely segregated into specific anatomical compartments (Swanson & Kuypers, 1980; Van den Pol, 1982; Swanson & Sawchenko, 1983). The parvocellular PVN cells are further categorized in different neuronal types, including neuroendocrine neurons that project to the median eminence and regulate the release of hormones from the anterior pituitary gland, and pre-autonomic neurons that send long descending projections to brainstem and spinal cord regions that are important with respect to autonomic control. The PaPo cells have been categorized as a parvocellular pre-autonomic PVN cells (Stern, 2001). Recent study demonstrated that the PaPo represented satiety-dependent cFos and oxytocin gene expressions (Uchoa et al., 2009), yet the neuronal circuits underlying satiety controls in the PaPo have not been clearly demonstrated.

The previous study of ours examined X-gal staining of broad hypothalamic areas of CCK1R^{+/-} mice and demonstrated high levels of staining signals in the hypothalamic PVN, particularly in the PaPo (Shimazoe et al., 2008). The present study further analyzed detailed

distribution of CCK-1 receptors in the hypothalamic PVN and demonstrated significant CCK-1 receptor density in the PaPo in comparison with anterior-to-medial PVN. The gradient in CCK-1 receptor expressions within the PVN was also supported by the real-time RT-PCR assay. Furthermore, Ca^{2+} imaging experiments demonstrate that distribution of functional CCK-1 receptors in accordance with the gene expression profiles. Koutcherov et al., (2000) analyzed structure of human hypothalamic PVN using immunohistochemistry and demonstrated significant levels of acetylcholine esterase expression in the PaPo. Consistently, we preliminary observed that about half of PaPo cells were carbachol responsive. However, carbachol responses rarely overlap to CCK-8s responses in the PaPo (data not shown), suggesting cholinergic and CCKergic cells are neighboring but distinct cell populations. It has shown that intravenous administration of CCK-8s elevated cFos expression in the oxytocin-secreting parvocellular neurons in the PVN and this response was absent in OLETF rats (Hashimoto et al., 2005). Therefore, oxytocin-positive but not cholinergic PaPo neurons possibly play a pivotal role for CCK-mediated satiety controls in the PVN.

Release of Ca^{2+} from internal Ca^{2+} stores via synergic activation of CCK-1 and -2 receptors in PaPo neurons

CCK-8s is a general CCK receptor agonist which has twice affinity to CCK-1 receptors than to CCK-2 receptors (Berna et al., 2007). CCK-8s sometimes described as a specific CCK-1 receptor agonist even with use at high concentrations (100-1,000 nM) for *in vitro* slices (Sorimachi et al., 2001). However, the present study carefully analyzed the dose-response curve both for the wild type and CCK1R^{-/-} slices and demonstrates that only low concentration (10 nM) CCK-8s is specific to mobilize Ca^{2+} via CCK-1 receptors. Concentration higher than 30 nM, however, mobilized Ca^{2+} both via CCK-1 and -2 receptors in PaPo cells.

CCK-1 and -2 receptors represent high structural homology and are both G_q protein-coupled receptors linking to phosphatidyl inositol cascade to mobilize Ca^{2+} from endoplasmic Ca^{2+} stores following activations (Kopin et al., 1992; Ulrich et al., 1993). Consistent with the theoretical signaling reported for model cells, the present study demonstrated Ca^{2+} mobilizations from internal Ca^{2+} stores both via CCK-1 and -2 receptors (i.e., low and high concentration CCK-8s) in PaPo cells. It has been shown that CCK-1 and -2 receptors could form hetero dimer which enhance signaling in CHO cell models (Cheng et al., 2003). Whether such synergic and direct interactions between two receptor subtypes could occur in the real biological system was not known, however. The present study demonstrated Ca^{2+} mobilizations via CCK-1 and -2 receptors in identical PaPo neurons in the wild type slice. The amplitudes of Ca^{2+} transients caused by co-stimulation of CCK-1 and -2 receptors were significantly larger than those via single subtype stimulations. This additive action obeys

implication in CHO cells which received double transfection of CCK-1 and -2 receptor genes (Cheng et al., 2003). Therefore, we assume synergic contribution of these two receptors for the CCK-mediated Ca^{2+} signaling in PaPo cells at least via pharmacological stimulations with CCK-8s, although the present study did not visualize sub-cellular localization of CCK-1 and -2 receptors.

Ablated CCK-1 receptor functions were compensated by CCK-2 receptor functions in CCK1R^{-/-} mice

The redundant CCK-1 and -2 receptor signaling in PaPo cells raised questions as to whether the co-stimulation of two receptor subtypes is essential for the endogenous CCK-mediated satiety controls. Because Gibbs et al., (1973) characterized CCK as a satiety factor and two CCK receptors were successfully cloned (Wank et al., 1992a, 1992b), specific CCK-receptor ligands to control satiety have been widely explored. It has been shown so far that reagents for CCK-1 receptors rather than for CCK-2 receptors successfully control satiety (Moran et al., 1992; Simmons et al., 1999). Therefore, it seems likely that preferential or larger contribution of CCK-1 receptor-mediated signaling for the endogenous satiety control. Interestingly, the present study revealed day-night differences in the Ca^{2+} mobilizations via CCK-1 receptors whereas no such differences were detected by co-stimulations of CCK-1 and -2 receptors. Thus, intrinsic CCK regulations such via circadian clock control of PVN axis (Aston-Jones et al., 2001) may be more closely associated with CCK-1 receptors.

Consistent with the accumulated pharmacological evidences, deletion in CCK-1 receptor genes was identified in OLETF rats (Takiguchi et al., 1997; Moran et al., 1998). However, involvement of CCK-1 receptors in regulation of satiety is currently controversial. For example, CCK1R^{-/-} mice do not develop hyperphagia and obesity when maintained on regular chow (Kopin et al., 1999; Takiguchi et al., 2002) despite the obvious obese phenotype of OLETF rats. Bi et al. (2004) demonstrated that OLETF rats had elevated neuropeptide Y mRNA expression in the DMH whereas this was not seen in CCK1R^{-/-} mice. Since CCK-1 receptors are co-localized with neuropeptide Y in the DMH of control strain rats (Bi et al., 2004) and knock down of neuropeptide Y in OLETF rats resulted in a significant reduction in body weight and food intake (Yang et al., 2009), the phenotypic discrepancy between rats and mice has been explained by the differential receptor expressions in the DMH and resultant uncoupling from neuropeptide Y signaling. However, Blevins et al. (2009) recently demonstrated that CCK-1 receptor knockout rats (F344, Cck1r^{-/-}) do not display obesity, similar to CCK1R^{-/-} mice, and thus it is also possible that the phenotype of OLETF rats depends on genes other than the CCK-1 receptor gene, which has been demonstrated previously (Muramatsu et al., 2005).

The present study demonstrated that deleted CCK-1 receptor functions were

replaceable by CCK-2 receptors in the CCK1R^{-/-} mice as (i) CCK-2 receptor transcriptions were upregulated in the PVN and NTS in CCK1R^{-/-} mice; (ii) a consistent increase in CCK2R protein level was found in the PVN of CCK1R^{-/-} mice; (iii) $\Delta[\text{Ca}^{2+}]_i$ following CCK-2 receptor stimulations were amplified in PaPo cells of CCK1R^{-/-} slices, and (iv) food intake behaviors were upregulated by CI-988 in CCK1R^{-/-} mice. The results showing compensatory functions between CCK-1 and -2 receptors thus may provide additional interpretation for the normal satiety controls in CCK1R^{-/-} mice. Recently, we found CCK-1 receptor expressions in the third ventricular ependymal cells at early developmental stages and its function for baby's suckling control (Ozaki et al., 2009). As in the adult PaPo cells, the neonatal third ventricular ependymal cells express both CCK-1 and -2 receptors whereas their functional compensation did not occur during early developmental stages. In fact, CCK1R^{-/-} pups displayed overweight phenotype regardless of maternal genotypes. Therefore, functional compensation between CCK-1 and -2 receptors may be processed during postnatal development.

Regular food intake activities and body weights are also reported for CCK null mutant mice (Lo et al., 2008). Therefore, functional compensation in molecules underlying CCK-mediated satiety controls may not be limited within two CCK receptor subtypes but also by other receptor signaling such via leptin (Wang et al., 2000; Li et al., 2011). For either case, results derived from the conventional knockout mice need careful interpretations to estimate single molecule functions within a system. Generation of conditional knockout mice such including Tet-On/Off systems will provide a better estimation for the net CCK functions for satiety controls. In conclusion, the present study characterized CCK receptor functions in the PVN and suggests functional compensation between CCK-1 and -2 receptors in PaPo cells which guarantees regular food intake behaviors.

FIGURE LEGENDS

Figure 1. A. X-gal staining of lacZ reporters expressed in CCK1R^{+/-} mouse brain sections. PVN, paraventricular nucleus; DMH, dorsal medial hypothalamus; ARC, arcuate nucleus; NTS, nucleus tractus solitaries; AP, area postrema; 3V, third ventricle. Bar = 200 μ m. **B.** Immunohistochemical identification of CCK-1 receptors in the hypothalamic PVN. *Upper.* The lacZ reporters stained with an antibody against β -galactosidase (β -gal) which visualized CCK-1 receptor gene expressions in CCK1R^{+/-} mice. *Lower.* The signal (colored as red) was superimposed on blue nuclear counter-staining by DAPI. The β -gal staining signals were localized in the posterior part of the PVN (PaPo). PaAP, paraventricular hypothalamic nucleus, anterior parvicellular part; PaV, paraventricular hypothalamic nucleus, ventral part; PaDC, paraventricular hypothalamic nucleus, dorsal cap; PaLM, paraventricular hypothalamic nucleus, lateral magnocellular part; PaMP, paraventricular hypothalamic nucleus, medial parvicellular part; PaMM, paraventricular hypothalamic nucleus, medial magnocellular part. Bar = 200 μ m. **C.** Number of β -gal-immunoreactive (ir) cells in anterior-to-posterior PVN was counted (n = 3). $**F_{2,6} = 349, P < .01$ compared to the anterior PVN by Duncan's multiple range tests following one way ANOVA. **D.** Field density of CCK-1 receptor expression was also calculated as the ratio of number of β -gal-ir cells per number of counter staining within the yellow dotted boundaries. $^{\#}F_{2,6} = 641, P < .01$ compared to the anterior- or the medial PVN by Duncan's multiple range tests following one way ANOVA.

Figure 2. Intracellular Ca²⁺ mobilizations in the hypothalamic PVN. A. The distribution of PVN cells showing a CCK-8s (10 nM)-induced Ca²⁺ increase under TTX perfusion was analyzed using sequential PVN slices. Slices from CCK1R^{-/-} mice (-/-) did not show CCK-8s (10 nM)-induced Ca²⁺ increases in any PVN subregion. There was a significantly larger responsive cell population in the posterior part of PVN as compared with the anterior or medial regions in wild-type slices (+/+). Six slices were used for each group. $**F_{2,15} = 63.41, P < .01$ as compared with the wild-type anterior PVN and $^{\#}F_{2,15} = 63.41, P < .01$ as compared with the wild-type medial PVN by Duncan's multiple range test following one-way ANOVA. **B.** Posterior PVN cells were repeatedly stimulated by different concentrations of CCK-8s to analyze dose responses. Representative cell responses in wild-type (+/+), heterozygous (+/-) and CCK1R^{-/-} (-/-) mice are shown. Note that CCK-8s (10 nM) increased intracellular Ca²⁺ levels in wild-type and heterozygous slices, but not in CCK1R^{-/-} slices. All experiments were conducted in the presence of 0.5 μ M TTX. Glutamic acid was applied at the end of experiments as a positive control. **C.** Dose-response curve for CCK-8s showing Ca²⁺ responsiveness. EC₅₀ was

estimated at 15.2 nM for wild-type cells and 48.7 nM for CCK1R^{-/-} cells. **D.** Responsive cell populations in wild-type PaPo slices were compared between daytime and nighttime. Six slices were used for each population analysis. *P<.05 by Student's t-test.

Figure 3. CCK-8s triggered release of Ca²⁺ from internal Ca²⁺ stores in PaPo cells both at low (10 nM) and high (100 nM) concentrations. **A.** the CCK-8s (10 nM; *arrows*)-induced Ca²⁺ mobilizations in wild-type PaPo cells. These responses were resistant to the replacement of normal extracellular buffer to Ca²⁺-free buffer (*left*) but were abolished following thapsigargin-induced depletion of internal Ca²⁺ stores (*right*). **B.** The CCK-8s (100 nM; *arrows*)-induced Ca²⁺ mobilizations in CCK1R^{-/-} (-/-) PaPo cells were resistant to the replacement of normal extracellular buffer with Ca²⁺-free buffer (*left*) but were abolished following thapsigargin-induced depletion of internal Ca²⁺ stores (*right*). All above responses were repeatedly observed in at least 30 cells in four slices. Of these, representative responses in three cells are plotted.

Figure 4. Pharmacological blockage of CCK-induced Ca²⁺ mobilizations in PaPo cells. **A. Left.** CCK-8s (10 nM)-induced Ca²⁺ mobilization in the wild type PaPo cells were reproducible at 25 min gaps. The second Ca²⁺ rises were blocked by CCK-1 receptor antagonist (LGM, 10 μM; *middle*) but were resistant to CCK-2 receptor antagonist (CI-988, 1 μM; *right*). **B. Left.** Specific CCK-2 receptor agonist, CCK-4 (100 nM) also evoked reproducible Ca²⁺ rise in the wild type PaPo cells at 25 min gaps. The second Ca²⁺ rises were blocked by CI-988 (1 μM; *right*) but were resistant to LGM (10 μM; *middle*). **C.** CCK-8s (100 nM)-induced Ca²⁺ mobilization in the wild type PaPo cells were reproducible at 25 min gaps (grey traces on *left*). The second Ca²⁺ rises were partially blocked by 10 μM LGM (*middle*) or by 1 μM CI-988 (*right*) whereas completely blocked by their commixtures (black traces on *left*). **D. Left.** Similar repeated Ca²⁺ mobilizations were produced by CCK-8s (100 nM) stimulations in PaPo cells of CCK1R^{-/-} mice (-/-). However, the second Ca²⁺ rises were resistant to LGM (10 μM; *middle*) but were abolished by CI-988 (1 μM, *right*). These results indicate that synergic contribution of CCK-1 and -2 receptors co-expressed in PaPo neurons determine the CCK-induced Ca²⁺ mobilization in PaPo cells. Representative responses in three cells were plotted.

Figure 5. Dose–response curves for CCK-8s-induced intracellular Ca²⁺ mobilizations in PaPo cells under treatments of CCK1R antagonist (LGM, 10 μM) or CCK2R antagonist (CI-988, 1 μM), with the experimental paradigm shown in Fig. 4, were analyzed. The dose–response curves were compared between the cells in wild-type (+/+) and CCK1R^{-/-} slices. All of the above responses were repeatedly observed in at least 30 cells in four slices.

Figure 6. CCK-1 and -2 receptor mRNA expressions in hypothetical centers for food intake and satiety controls. Relative CCK-1 and -2 receptor mRNA expressions were quantified as a function of housekeeping gene expression using a real-time RT-PCR. The relative abundance of CCK-1 and -2 receptor mRNA were analyzed for PVN subregions (**A**) and the other nuclei controlling food intake behaviors (**B**). Analysis for the caudate putamen (Cpu) was also examined as a negative control for CCK-1 receptor gene expressions. DMH, dorsal medial hypothalamus; VMH, ventral medial hypothalamus; Arc, arcuate nucleus; NTS, nucleus tractus solitaries. * $P < .05$; ** $P < .01$ by Student's t -test. #Largest CCK-1 receptor expressions in comparison with other brain areas ($F_{6,21} = 6.1$, $P < .01$ by one way ANOVA). Four tissue punch-outs were used to calculate average.

Figure 7. A. The distribution of CCK1R and -2R proteins in the PaPo was analyzed by immunofluorescence double labeling and confocal microscopy. CCK1R (green), CCK2R (red), and DAPI nuclear staining (blue) were superimposed on the merged color images. Note that most of the CCK1R signals overlapped the CCK2R signals, resulting in the yellow color in the CCK1R-positive cells in the wild-type slice (+/+). Negligible staining levels for CCK1R were found in the CCK1R-/- slice (-/-). **B.** CCK2R protein abundance in the hypothalamus was further quantified using western blotting. Relative abundance of CCK2R protein in PVN was larger in the CCK1R-/- mice (-/-) than in the wild-type mice (+/+). Corresponding differences were not detectable in the DMH or in any of the VMH and ARC regions. ** $P < .01$ by Student's t -test. Four samples were used to calculate the average.

Figure 8. A. Injection of LGM (2 mg/kg *i.p.* at dark onset) upregulated food accesses in the wild type (+/+) but not in CCK1R-/- mice (-/-). Grey area plot denotes number of food accesses after vehicle injection one day before LGM injection. Black area plot denotes number of food accesses after LGM injection. $n = 8$ for each genotype. **B.** Injection of CI-988 (2 mg/kg, *i.p.* at dark onset) rather increased food accesses in CCK1R-/- mice (-/-) but not in the wild type mice (+/+). Grey and black area plots denote vehicle- and CI-988 injected groups, respectively. $n = 6$ for each genotype. * $P < .05$ by Student's t -test in comparison with corresponding vehicle-injected controls. Black and white bars on the bottom denote light and dark period. **C.** The 12-h cumulative number of food accesses following the LGM injection was calculated for further comparisons between genotypes. **D.** The 12-h cumulative number of food accesses following injection of CI-988 injection was also analyzed. * $P < .05$; ** $P < .01$ by one way repeated ANOVA. Reference dotted lines denote levels of 12-h cumulative number of food accesses in vehicle-injected wild type mice which were equivalent for those in vehicle-injected CCK1R-/- mice.

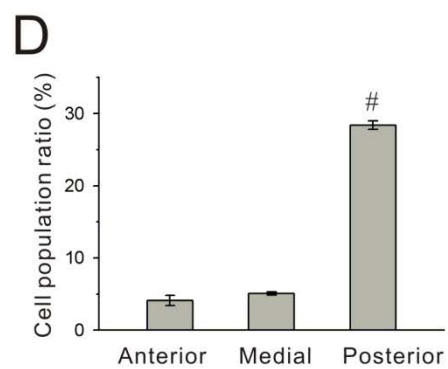
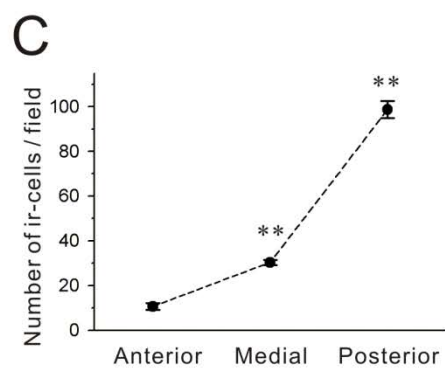
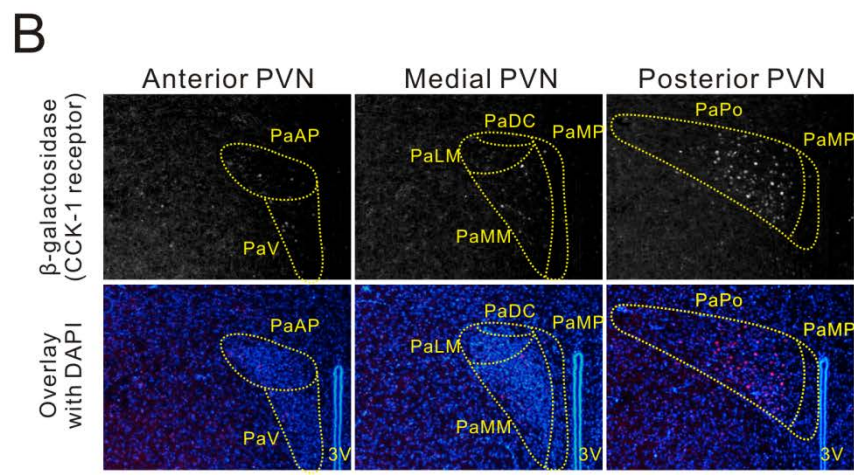
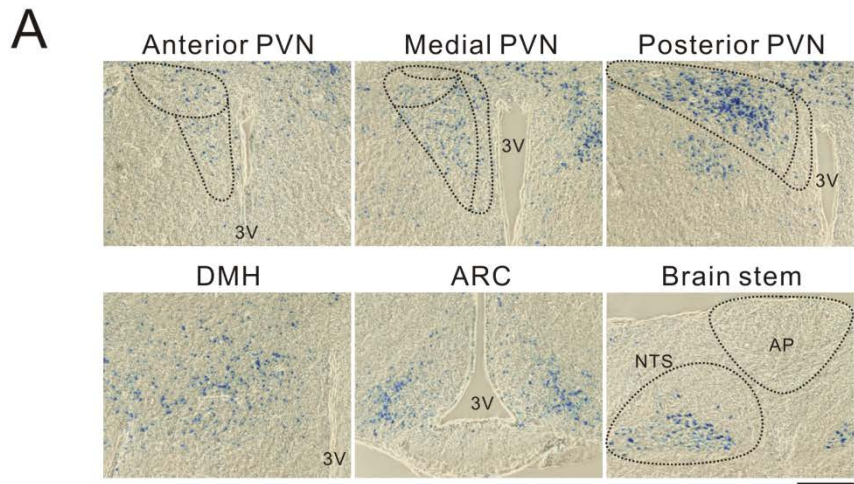


Figure 1

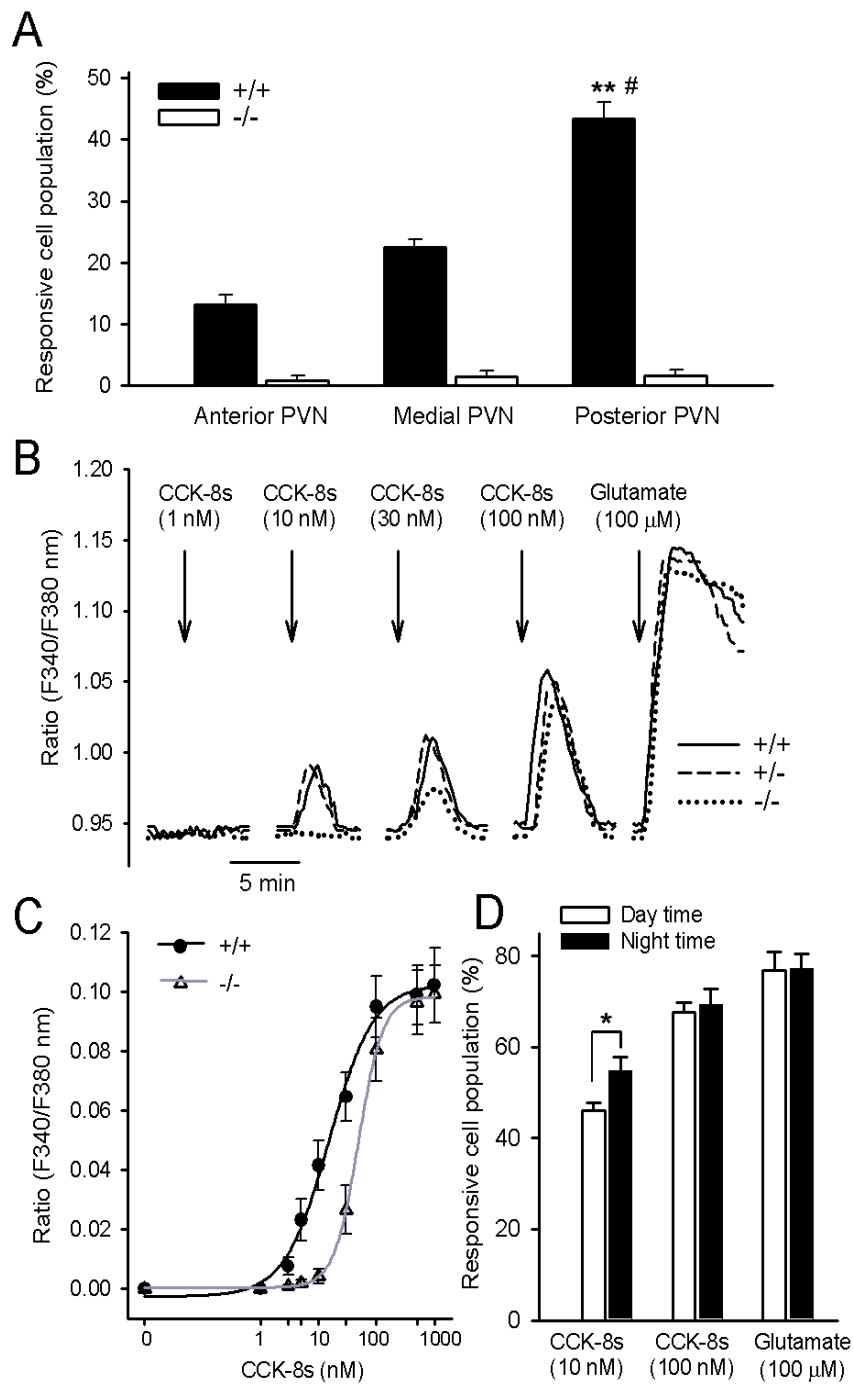


Figure 2

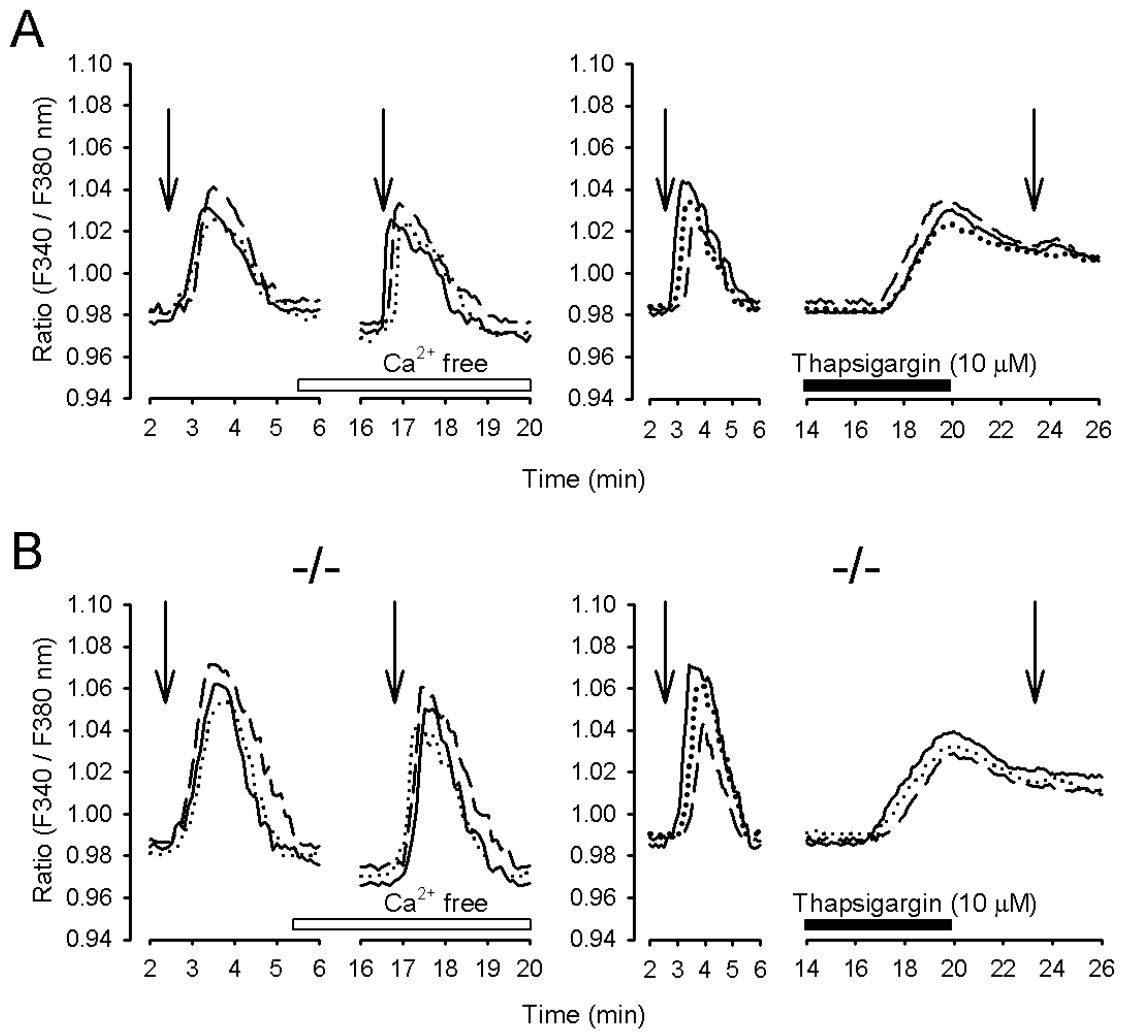


Figure 3

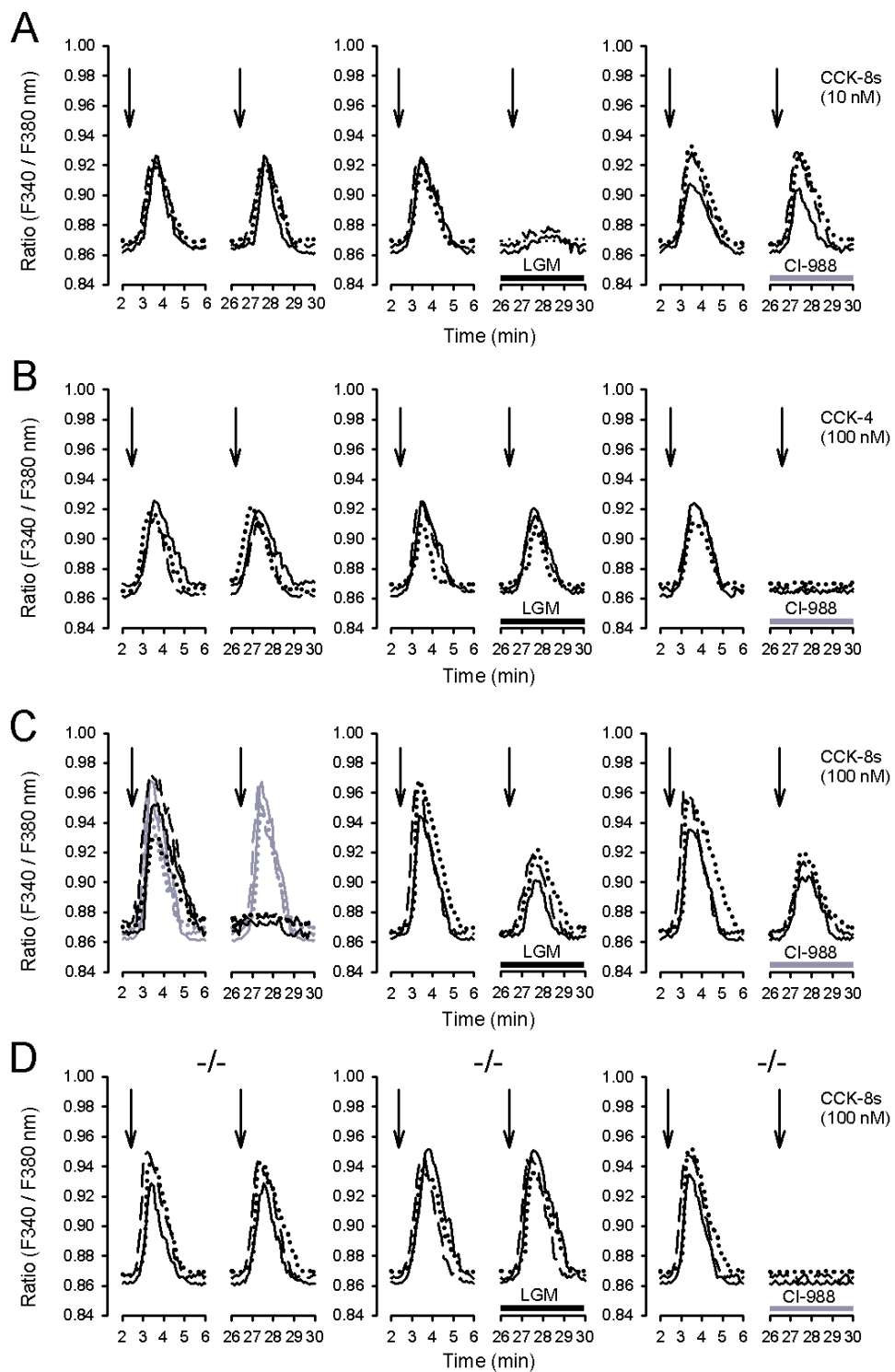


Figure 4

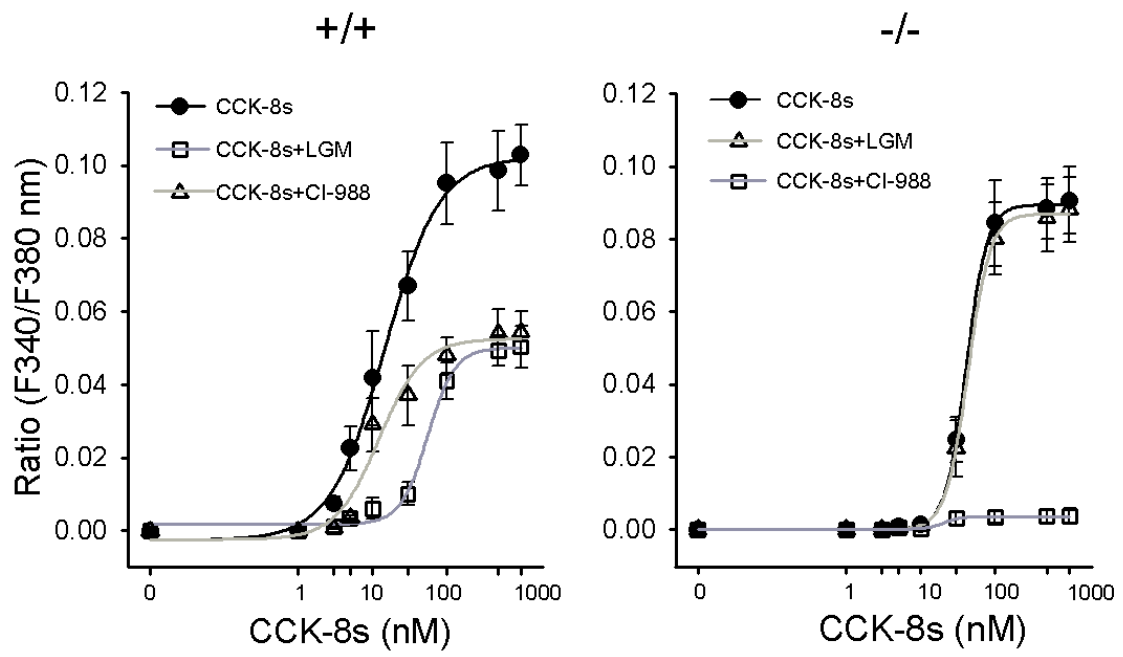


Figure 5

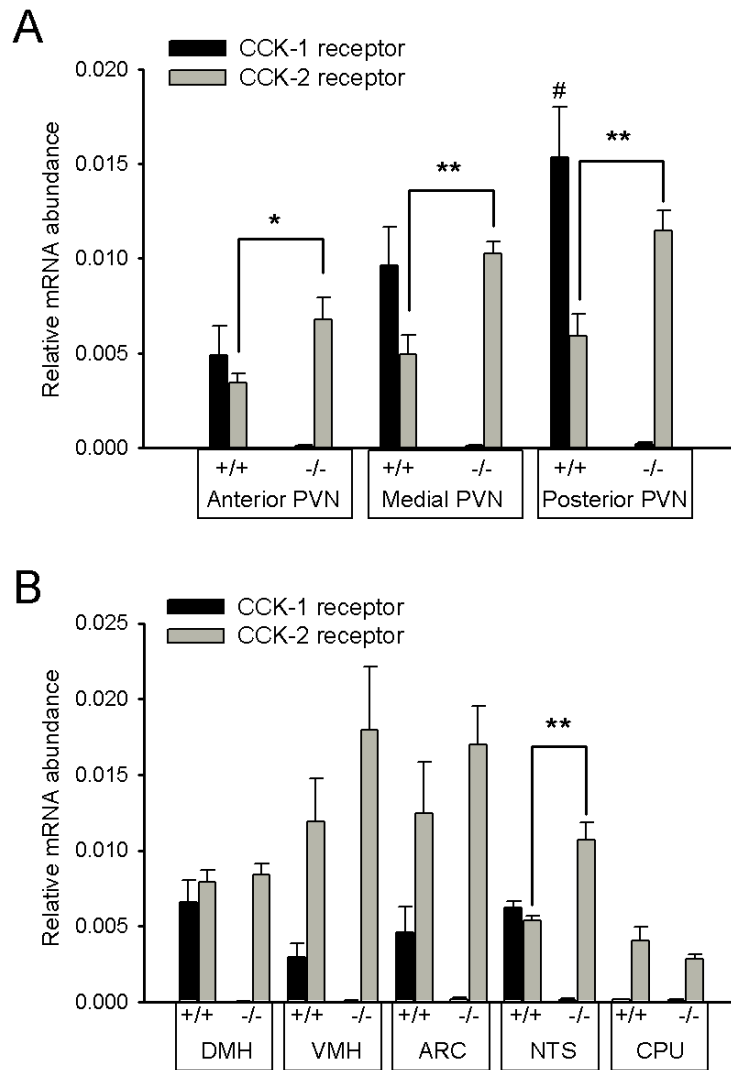


Figure 6

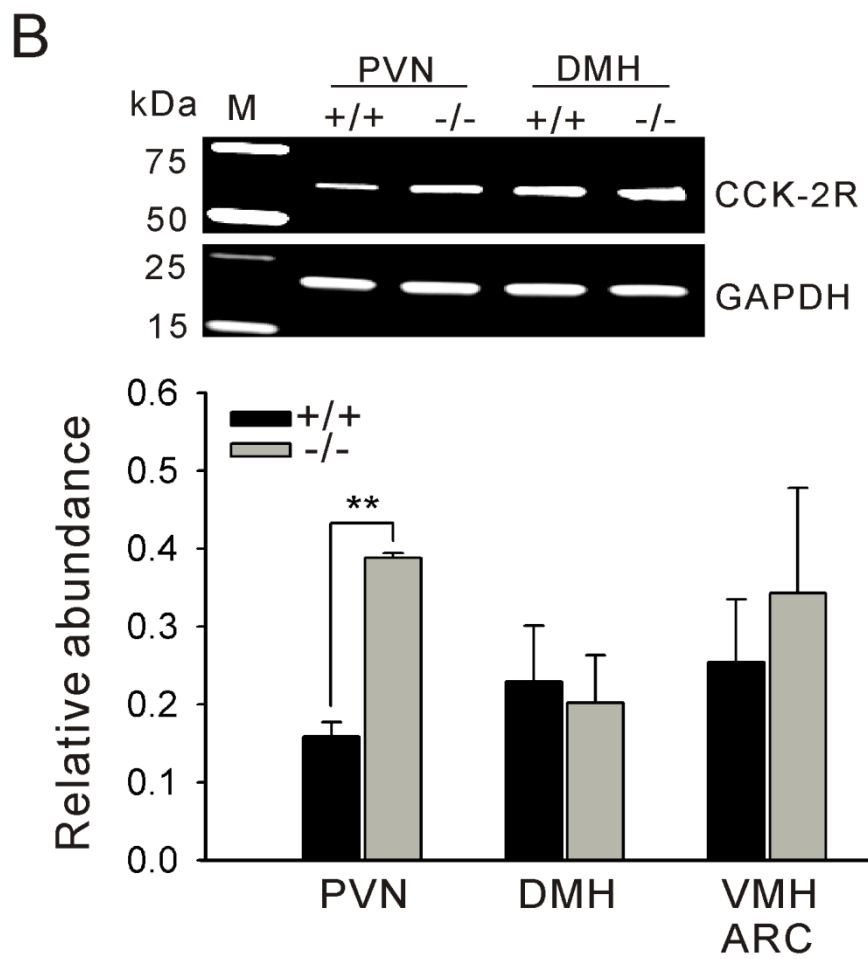
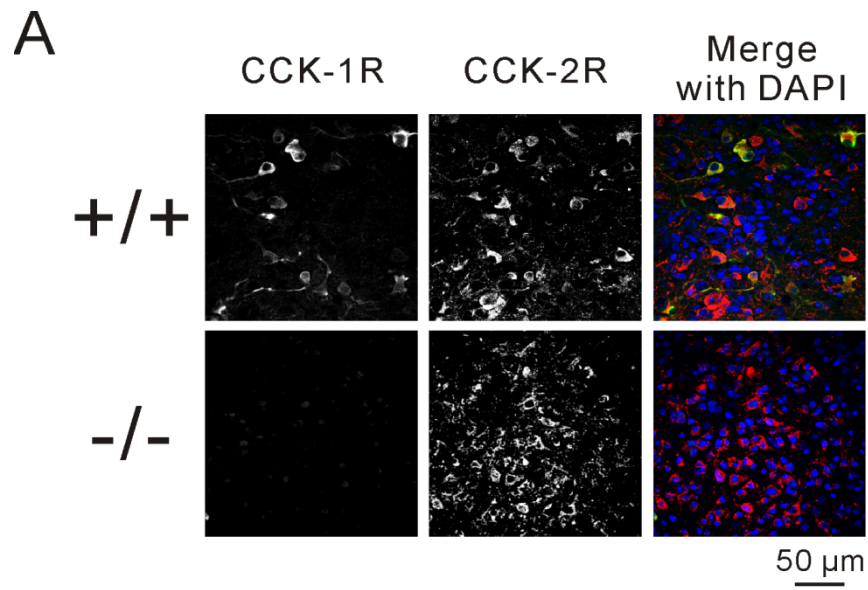


Figure 7

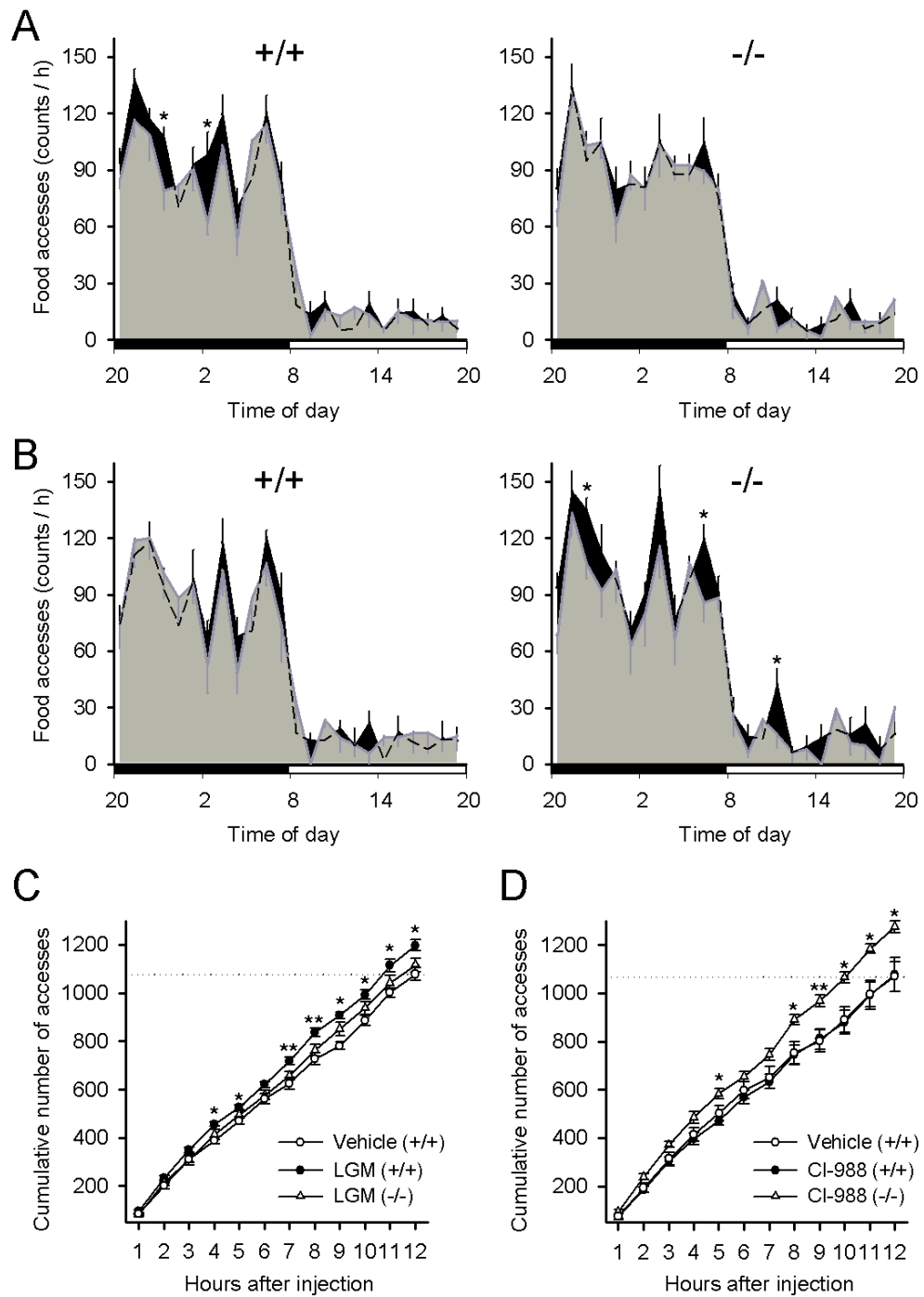


Figure 8

REFERENCE

1. Aston-Jones, G., Chen, S., Zhu, Y., and Oshinsky, M. L. (2001) *Nat. Neurosci.* **4**, 732-738
2. Appleyard, S. M., Marks, D., Kobayashi, K., Okano, H., Low, M. J., and Andresen, M. C. (2007) *J. Neurosci.* **27**, 13292-13302
3. Antin, J., Gibbs, J., Holt, J., Young, R. C., and Smith, G. P. (1975) *J. Comp. Physiol. Psychol.* **89**, 784-790
4. Baber, N. S., Dourish, C. T., and Hill, D. R. (1989) *Pain* **39**, 307-328
5. Berna, M. J., Tapia, J. A., Sancho, V., and Jensen, R. T. (2007) *Curr. Opin. Pharmacol.* **7**, 583-592
6. Bi, S., Scott, K. A., Kopin, A. S., and Moran, T. H. (2004) *Endocrinology* **145**, 3873-3880
7. Blevins, J. E., Overduin, J., Fuller, J. M., Cummings, D. E., Matsumoto, K., and Moralejo, D. H. (2009) *Brain Res.* **1255**, 98-112
8. Bondy, C. A., Whitnall, M. H., Brady, L. S., and Gainer, H. (1989) *Cell. Mol. Neurobiol.* **9**, 427-446
9. Broberger, C., Holmberg, K., Shi, T. J., Dockray, G., and Hökfelt, T. (2001) *Brain Res.* **903**, 128-140
10. Cawston, E. E., and Miller, L. J. (2010) *Br. J. Pharmacol.* **159**, 1009-1021
11. Cheng, Z. J., Harikumar, K. G., Holicky, E. L., and Miller, L. J. (2003) *J. Biol. Chem.* **278**, 52972-52979
12. Crawley, J. N., Fiske, S. M., Durieux, C., Derrien, M., and Roques, B. P. (1991) *J. Pharmacol. Exp. Ther.* **257**, 1076-1080
13. Gibbs, J., Young, R. C., and Smith, G. P. (1973) *Nature* **245**, 323-325
14. Guard, D. B., Swartz, T. D., Ritter, R. C., Burns, G. A., and Covasa, M. (2009) *Brain Res.* **1266**, 37-44
15. Hashimoto, H., Onaka, T., Kawasaki, M., Chen, L., Mera, T., Soya, A., Saito, T., Fujihara, H., Sei, H., Morita, Y., and Ueta, Y. (2005) *Auton. Neurosci.* **121**, 16-25
16. Hinks, G. L., Poat, J. A., and Hughes, J. (1995) *Neuroscience* **68**, 765-781
17. Hirose, Y., Inui, A., Teranishi, A., Miura, M., Nakajima, M., Okita, M., Nakajima, Y., Himori, N., Baba, S., Kasuga, M. (1993) *Am. J. Physiol.* **265**, R481-R486
18. Honda, T., Wada, E., Battey, J. F., and Wank, S. A. (1993) *Brain. Mol. Cell. Neurosci.* **4**, 143-154
19. Itoh, S., and Lal, H. (1990) *Drug. Dev. Res.* **21**, 257-276
20. Ivy, A. C., and Oldberg, E. (1928) *Am. J. Physiol.* **86**, 599-613
21. Kiyama, H., Shiosaka, S., Kubota, Y., Cho, H. J., Takagi, H., Tateishi, K., Hashimura, E., Hamaoka, T., and Tohyama, M. (1983) *Neuroscience* **10**, 1341-1359

22. Kopin, A. S., Lee, Y. M., McBride, E. W., Miller, L. J., Lu, M., Lin, H.Y., Kolakowski, L. F. Jr., and Beinborn, M. (1992) *Proc. Natl. Acad. Sci. U. S. A.* **89**, 3605-3609
23. Kopin, A. S., Mathes, W. F., McBride, E. W., Nguyen, M., Al-Haider, W., Schmitz, F., Bonner-Weir, S., Kanarek, R., and Beinborn, M. (1999) *J. Clin. Invest.* **103**, 383-391
24. Koutcherov, Y., Mai, J. K., Ashwell, K. W., and Paxinos, G. (2000) *J. Comp. Neurol.* **423**, 299-318
25. Li, Y., Wu, X., Zhou, S., and Owyang, C. (2011) *Am. J. Physiol. Gastrointest. Liver Physiol.* **300**, G217-G227
26. Lo, C. M., Samuelson, L. C., Chambers, J. B., King, A., Heiman, J., Jandacek, R. J., Sakai, R. R., Benoit, S. C., Raybould, H. E., Woods, S. C., and Tso, P. (2008) *Am. J. Physiol.* **294**, R803-R810
27. Mönnikes, H., Lauer, G., Bauer, C., Tebbe, J., Zittel, T. T., and Arnold, R. (1997) *Am. J. Physiol.* **273**, R2059-R2071
28. Moran, T. H., Ameglio, P. J., Schwartz, G. J., and McHugh, P. R. (1992) *Am. J. Physiol.* **262**, R46-R50
29. Moran, T. H., Katz, L. F., Plata-Salaman, C. R., and Schwartz, G. J. (1998) *Am. J. Physiol.* **274**, R618-R625
30. Muramatsu, Y., Yamada, T., Taniguchi, Y., Ogini, T., Kose, H., Matsumoto, K., Sasaki, Y. (2005) *Biochem. Biophys. Res. Commun.* **331**, 1270-1276
31. Mutt, V., and Jorpes, J. E. (1968) *Eur. J. Biochem.* **6**, 156-162
32. Ozaki, T., Takiguchi, S., and Ikeda, M. (2009) *J. Physiol. Sci.* **59**, (Suppl) 461
33. Panicker, A. K., Mangels, R. A., Powers, J. B., Wade, G. N., and Schneider, J. E. (1998) *Am. J. Physiol.* **275**, R158-R164
34. Raboin, S. J., Reeve, Jr. J. R., Cooper, M. S., Green, G. M., and Sayegh, A. I. (2008) *Regul. Pept.* **150**, 73-80
35. Reidelberger, R. D., Heimann, D., Kelsey, L., and Hulce, M. (2003) *Am. J. Physiol.* **284**, R389-R398
36. Reidelberger, R. D., Hernandez, J., Fritzsich, B., and Hulce, M. (2004) *Am. J. Physiol.* **286**, R1005-R1012
37. Rinaman, L., Verbalis, J. G., Stricker, E. M., and Hoffman, G. E. (1993) *J. Comp. Neurol.* **338**, 475-490
38. Shimazoe, T., Morita, M., Ogiwara, S., Kojiya, T., Goto, J., Kamakura, M., Moriya, T., Shinohara, K., Takiguchi, S., Kono, A., Miyasaka, K., Funakoshi, A., and Ikeda, M. (2008) *FASEB J.* **22**, 1479-1490
39. Silver, R., Sookhoo, A. I., LeSauter, J., Stevens, P., Jansen, H. T., and Lehman, M. N. (1999) *Neuroreport* **10**, 3165-3174

40. Simmons, R. D., Kaiser, F. C., and Hudzik, T. J. (1999) *Pharmacol. Biochem. Behav.* **62**, 549-557
41. Smith, G. P., Jerome, C., Cushin, B. J., Eterno, R., and Simansky, K. J. (1981) *Science* **213**, 1036-1037
42. Smith, G. P., Jerome, C., and Norgren, R. (1985) *Am. J. Physiol.* **249**, R638-R641
43. Sorimachi, M., Yamagami, K., and Uramura, K. (2001) *Neurosci. Lett.* **300**, 91-94
44. Stern, J. E. (2001) *J. Physiol.* **537**, 161-177
45. Swanson, L. W., Kuypers, H. G. (1980) *J. Comp. Neurol.* **194**, 555-570
46. Swanson, L. W., and Sawchenko, P. E. (1980) *Neuroendocrinology* **31**, 410-417
47. Swanson, L. W., and Sawchenko, P. E. (1983) *Annu. Rev. Neurosci.* **6**, 269-324
48. Szewczyk, J. R., and Laudeman, C. (2003) *Curr. Top. Med. Chem.* **3**, 837-854
49. Takagi, H., Mizuta, H., Matsuda, T., Inagaki, S., Tateishi, K., and Hamaoka, T. (1984) *Brain Res.* **309**, 346 -349
50. Takiguchi, S., Takata, Y., Funakoshi, A., Miyasaka, K., Kataoka, K., Fujimura, Y., Goto, T., and Kono, A. (1997) *Gene* **197**, 169-175
51. Takiguchi, S., Suzuki, S., Sato, Y., Kanai, S., Miyasaka, K., Jimi, A., Shinozaki, H., Takata, Y., Funakoshi, A., Kono, A., Minowa, O., Kobayashi, T., and Noda, T. (2002) *Pancreas* **24**, 276-283
52. Uchoa, E. T., Mendes da Silva, L. E., de Castro, M., Antunes-Rodrigues, J., and Elias, L. L. (2009) *Horm. Behav.* **56**, 532-538
53. Ulrich, C. D., Ferber, I., Holicky, E., Hadac, E., Buell, G., and Miller, L. J. (1993) *Biochem. Biophys. Res. Commun.* **193**, 204-211
54. Van den Pol, A. N. (1982) *J. Comp. Neurol.* **206**, 317-345
55. Van den Pol, A. N., and Tsujimoto, K. L. (1985) *Neuroscience* **15**, 1049-1086
56. Wank, S. A., Harkins, R., Jensen, R. T., Shapira, H., de Weerth, A., and Slattery, T. (1992a) *Proc. Natl. Acad. Sci. U. S. A.* **89**, 3125-3129
57. Wank, S. A., Pisegna, J. R., and de Weerth, A. (1992b) *Proc. Natl. Acad. Sci. U. S. A.* **89**, 8691-8695
58. Wang, L., Barachina, M. D., Martínez, V., Wei, J. Y., and Tache, Y. (2000) *Regul. Pept.* **92**, 79-85
59. Washington, M. C., Murry, C. R., Raboin, S. J., Roberson, A. E., Mansour, M. M., Williams, C. S., and Sayegh, A. I. (2010) *Peptides* **32**, 272-280
60. Wei, J. Y., and Wang, Y. H. (2000) *Am. J. Physiol.* **279**, E695-E706
61. Yang, L., Scott, K. A., Hyun, J., Tamashiro, K. L., Tray, N., Moran, T. H., and Bi, S. (2009) *J. Neurosci.* **29**, 179-190